THE HOST GALAXY OF GRB 980703 AT RADIO WAVELENGTHS — A NUCLEAR STARBURST IN A ULIRG

E. BERGER[1], S. R. KULKARNI[1], D. A. FRAIL[2]

Draft version May 7, 2001

ABSTRACT

We present radio observations of GRB 980703 at 1.43, 4.86, and 8.46 GHz for the period of 350 to 1000 days after the burst. These radio data clearly indicate that there is a persistent source at the position of GRB 980703 with a flux density of approximately 70 μJy at 1.43 GHz, and a spectral index, $\beta \approx 0.32$, where $F_\nu \propto \nu^{-\beta}$. We show that emission from the afterglow of GRB 980703 is expected to be one to two orders of magnitude fainter, and therefore cannot account for these observations. We interpret this persistent emission as coming from the host galaxy — the first example of a γ-ray burst (GRB) host detection at radio wavelengths. We show that emission from an AGN is unlikely, and find that it can be explained as a result of a star-formation rate (SFR) of massive stars ($M > 5$ $M_\odot$) of ≈ 90 $M_\odot$/yr, which gives a total SFR (0.1$M_\odot$ <M< 100$M_\odot$) of ≈ 500 $M_\odot$/yr. Using the correlation between the radio and far-IR (FIR) luminosities of star-forming galaxies, we find that the host of GRB 980703 is at the faint end of the class of Ultra Luminous Infrared Galaxies (ULIRGs), with $L_{FIR} \sim few \times 10^{12}$ $L_\odot$. From the radio measurements of the offset between the burst and the host, and the size of the host, we conclude that GRB 980703 occurred near the center of the galaxy in a region of maximum star formation. A comparison of the properties of this galaxy with radio and optical surveys at a similar redshift ($z \approx 1$) reveals that the host of GRB 980703 is an average star-forming galaxy. This result has significant implications for the potential use of a GRB-selected galaxy sample for the study of galaxies and the IGM at high redshifts, especially using radio observations, which are insensitive to extinction by dust and provide an unbiased estimate of the SFR through the well-known radio-FIR correlation.

Subject headings: gamma rays:bursts – radio continuum:general – cosmology:observations – galaxies:starburst – stars:formation

1. INTRODUCTION

Recent studies of the properties and host galaxies of γ-ray bursts (GRBs) reveal some indirect evidence for the link between GRBs and star formation. Optical measurements of the offset distribution of GRBs from their host centers appears to be consistent with the distribution of collapsars in an exponential disk, but inconsistent with the expected offset distribution of delayed binary mergers (Bloom, Kulkarni & Djorgovski 2001). GRB 990705 is an illustrative example of this result since HST images revealed that the burst was situated in a spiral arm, just north of an apparent star forming region (Holland et al. 2000; Bloom, Kulkarni & Djorgovski 2001). The absence of optical afterglows from the so-called "dark GRBs" (Djorgovski et al. 2001) points to the association of GRBs with heavily obscured, and possibly star-forming, regions. In addition, Galama & Wijers (2000) claim high column densities toward several GRBs from X-ray observations of afterglows

Consequently, one of the pressing questions in the study of GRB host galaxies is whether they are representative of star-forming galaxies at a similar redshift. If they are, then the dust-penetrating power of GRBs and their broadband afterglow emission offer a number of unique diagnostics of their host galaxies: the obscured star formation fraction, the ISM within the disk, the local environment of the burst itself, and global and line-of-sight extinction, to name a few.

GRB 980703, which has one of the brightest (apparent magnitude) hosts to date ($R \approx 22.6$ mag; Bloom et al. 1998; Vreeswijk et al. 1999) offers an excellent opportunity for detailed studies. The afterglow optical and near-IR (NIR) lightcurves exhibited pronounced flattening about 6 days after the burst and this was attributed to an underlying bright host (Bloom et al. 1998; Castro-Tirado et al. 1999; Vreeswijk et al. 1999). Djorgovski et al. (1998) undertook spectroscopic observations of the host and obtained a redshift of 0.966. Using three different estimators ([OII], Hα and 2800A UV continuum) of the star-formation rate (SFR), Djorgovski et al. (1998) inferred extinction-corrected SFR of 10 to 30 $M_\odot$/yr.

Here we report radio observations of GRB 980703 covering the period 350–1000 days after the burst at three frequencies: 1.43, 4.86, and 8.46 GHz. This burst has the distinction of being followed up for 1000 days; the previous record-holder was GRB 970508 (445 days; Frail, Waxman & Kulkarni 2000). The organization of the paper is as follows. We summarize the radio observations and data reduction in §2. In §3 we show that the late time radio observations require a steady component over and above the decaying afterglow observations. We argue that this component is unlikely to arise from an AGN but is instead due to star-formation. In §4, we infer the SFR from the radio observations and compare and contrast this estimate to those derived from optical observations. Thanks to the high angular resolution and accurate astrometry of radio observations we are able to derive an accurate offset between the burst and the centroid of the host, as well as constrain the size of the radio emitting region (§5).

[1]Division of Physics, Mathematics, and Astronomy, California Institute of Technology 105-24, Pasadena, CA 91125

[2]National Radio Astronomy Observatory, P. O. Box O, Socorro, NM 87801

2. RADIO OBSERVATIONS

Very Large Array (VLA[3]) observations of GRB 980703 were initiated on 1998, July 4.40 UT at 4.86 GHz. All observations were obtained in the standard continuum mode with 2×50 MHz contiguous bands. We used the extra-galactic sources J2330+110, J0010+109 and J0022+061 for phase calibration and 3C48 (J0137+331) and 3C147 (J0542+498) for flux calibration. We used the Astronomical Image Processing System (AIPS) for data reduction. The fluxes presented here are the values measured on the images at the position of the source.

Late-time observations (time after the burst, $t \gtrsim 350$ days) were co-added over a period of a few to thirty days in order to increase the overall sensitivity of each detection. This is appropriate since the expected change in the flux density from the afterglow over a few days, several hundred days after the burst, is negligible relative to the associated errors in the measurements. A log of the late-time observations and the flux density measurements are summarized in Table 1, and the lightcurves are shown in Figure 1. A summary of the early radio data, as well as broadband modeling is given in Berger et al. (2001).

3. EVIDENCE FOR HOST GALAXY EMISSION IN THE RADIO REGIME

From Figure 1, we see that the late-time ($t \gtrsim 350$ days) radio lightcurves do not exhibit the customary power-law decay expected of afterglows but instead show flattening. From the early broadband data we know that the afterglow spectrum peaked at frequency, $\nu_m \sim 4 \times 10^{12}$ Hz at $t = 1.2$ days (Vreeswijk et al. 1999). If the explosion was spherical then we expect $\nu_m \propto t^{-3/2}$ (Sari, Piran & Narayan 1998; Chevalier & Li 2000). Thus the radio afterglow is expected to decay for $t > 70$ days after the burst. If the ejecta were collimated (opening angle, θ_j), then we expect a more rapid decay, $\nu_m \propto t^{-2}$, once the bulk Lorentz factor, Γ, of the flow falls below θ_j, $\Gamma(t) \lesssim \theta_j^{-1}$ (Sari, Piran & Halpern 1999). In this case, we expect the radio afterglow to start decaying at even earlier times, and the flux will decay faster relative to a spherical explosion. In either case, we expect the radio afterglow to decay by at least a factor of three over the time span under consideration, $350 < t < 1000$ days.

We can clearly see from Figure 1 that this decay is not taking place, and the flux instead remains constant over a period of approximately 650 days. This behavior is similar to the flattening observed in the optical/NIR lightcurves of several GRBs (including GRB 980703), when the emission from the afterglow decays below the level of emission from the host galaxy.

Furthermore, the afterglow spectrum is expected to be a power law, $F_\nu \propto \nu^{-\beta}$, where $\beta = (p-1)/2$ and p is the power law index of the Lorentz factor distribution of the shocked electrons, $N(\gamma)d\gamma \propto \gamma^{-p}d\gamma$ for $\gamma > \gamma_{\rm min}$ (Sari, Piran & Narayan 1998). From the observations of many afterglows, we note that p is in the range 2.2–2.6 and thus we expect $\beta \sim 0.7$. However, the observed spectral index in the range 1.43–8.46 GHz is much lower, $\beta = 0.32 \pm 0.12$. We thus conclude that there exists a steady source of emission other than the afterglow.

One possible explanation for this component is emission from an active galactic nucleus (AGN). It has been noted in surveys of the Hubble Deep Field (HDF), its flanking fields, and the Small Selected Area 13 (SSA13) that approximately 20% of the radio sources are AGN with spectral indices of about 0.3 (Richards et al. 1999; Richards 2000; Barger, Cowie & Richards 2000). Windhorst et al. (1993) found a similar result in their survey of two $7' \times 7'$ fields at 8.44 GHz. Thus, there is a modest probability that the emission from the host of GRB 980703 is due to an AGN.

We consider the AGN hypothesis unlikely based on the radio data and optical spectroscopy. First, optical spectra of the source obtained by Djorgovski et al. (1998) show no evidence for an unobscured AGN: high-ionization lines such as Mg II λ2799, [NeV]λ3346, and [NeV]λ3426 are absent, and the [OIII]λ4959 to Hβ ratio is approximately 0.4, much lower than [OIII]/H$\beta > 1.3$ for AGN (Rola, Terlevich & Terlevich 1997). Another way to discriminate between AGN and star-forming galaxies is to correlate the [OII] equivalent width (EW) with continuum color (Dressler & Gunn 1982). Kennicutt (1992) showed that AGN have redder colors for similar [OII] EW, relative to normal galaxies. Using the spectrum presented in Djorgovski et al. (1998) we evaluate the color index, $(41-50) \equiv 2.5\log[f_\nu(5000{\rm A})/f_\nu(4100{\rm A})]$ (Kennicutt 1992), and find it to be 0 ± 0.1; an AGN with the same [OII] EW would have a value $\gtrsim 0.3$ (Kennicutt 1992). Finally, Rola, Terlevich & Terlevich (1997) found that for a sample of emission-line galaxies at $z \sim 0.8$, the color index between the continuum underlying the Hβ and [OII]λ3727 lines is ≥ 0.4 for all AGN in their sample. Using the spectrum of Djorgovski et al. (1998) we find that this color index is approxmiately zero.

A second, but less persuasive argument against an AGN origin is the apparent absence of significant radio variability over the 650 day monitoring period (see Figure 2). The radio cores of most, but not all, low-luminosity AGN show variability exceeding the observed levels (Falcke et al. 2000).

We thus conclude that the radio emission seen from the host of GRB 980703 is unlikely to be due to AGN activity. However, star-forming galaxies exhibit radio emission arising from their supernova remnants (SNRs) and HII regions. In the next section we show how the observations, the radio spectral index, and the optical spectrum, are consistent with the hypothesis that the radio emission is related to star formation.

4. THE STAR-FORMATION RATE IN THE HOST GALAXY OF GRB 980703

Star formation is traced by optical, far-IR, sub-mm, and radio emission. In the following we will use the radio data to estimate the SFR in the host galaxy of GRB 980703, and then compare the results with the SFR derived from optical indicators, and with radio surveys at a similar redshift range in order to place the host of GRB 980703 in a larger context.

4.1. *Star Formation Rate from the Radio Observations*

Using all the measurements in Table 1, we find the following weighted-average flux densities for the host galaxy of GRB 980703: $F_{\nu,8.46} = 39.3 \pm 4.9$ μJy, $F_{\nu,4.86} = 42.1 \pm 8.6$ μJy, and $F_{\nu,1.43} = 68.0 \pm 6.6$ μJy. From the redshift of GRB 980703, $z = 0.966$ (Djorgovski et al. 1998), and the cosmological parameters $\Omega_0 = 0.3$, $\Lambda_0 = 0.7$ and $H_0 = 65$ km/sec/Mpc, we find that the luminosity distance to the burst is $d_L = d_A(1+z)^2 \approx 2.1 \times 10^{28}$ cm, and the observed luminosity at each frequency is given by $L_\nu = 4\pi d_L^2 F_\nu$. The emitted luminosity is given by

[3]The VLA is operated by the National Radio Astronomy Observatory (NRAO), a facility of the National Science Foundation operated under cooperative agreement by Associated Universities, Inc.

$L_{em,\nu'} = L_{obs,\nu}(\nu/\nu')^{\beta}(1+z)^{\beta}$, where β is the spectral index of the radio emission, ν' is the rest frequency, and ν is the observing frequency. From the flux densities we find that the radio spectral index is $\beta = 0.32 \pm 0.12$, and thus the emitted luminosity in each frequency is approximately 25% higher than the observed luminosity at the same frequency.

Condon (1992) showed that the total luminosity is a combination of synchrotron and thermal emission components, both directly related to the formation rate of massive stars via a simple relationship. Moreover, since the lifetime of massive stars is of the order of 10^7 years, and the lifetime of the synchrotron emitting electrons is of the order of 10^8 years (Condon 1992), the radio emission is an excellent probe of the instantaneous SFR. Using the emitted luminosity at $\nu' = 1.43$ GHz, $L_{em}(1.43) = (4.7 \pm 0.6) \times 10^{30}$ erg sec^{-1}, we find that the SFR of massive stars in the host of GRB 980703 is

$$\mathrm{SFR}(\mathrm{M}>5\mathrm{M}_{\odot}) \approx \frac{L_{em}(1.43)}{5.3\times10^{28}\nu'^{-\beta}_{\mathrm{GHz}}+5.5\times10^{27}\nu'^{-0.1}_{\mathrm{GHz}}} \approx 90\mathrm{M}_{\odot}/\mathrm{yr}. \quad (1)$$

Since both the thermal and non-thermal components are proportional only to the formation rate of high-mass stars, equation 1 has to be modified by a factor which accounts for the contribution from stars in the mass range 0.1–5 $\mathrm{M}_{\odot}$. For a Salpeter IMF this factor evaluates to 5.5. We use the Salpeter IMF since it is already implicitly used in equation 1 for the mass range 5–100 $\mathrm{M}_{\odot}$. Thus, within this framework the total SFR is ≈ 500 $\mathrm{M}_{\odot}$/yr.

We now compare the SFR and other characteristics of the host of GRB 980703 with those of other galaxies at a similar redshift. A radio survey of the Hubble Deep Field (HDF) and its flanking fields showed that the mean spectral index of the 8.46 GHz selected sample is $\langle\beta_{8.46}\rangle = 0.35 \pm 0.07$ (Richards 2000). In a survey of two $7' \times 7'$ fields with the VLA at 8.44 GHz Windhorst et al. (1993) found for sources with a flux density $\lesssim 100$ μJy (hereafter, μJy sources) a median spectral index, $\beta_{\mathrm{med}} \approx 0.35 \pm 0.15$, and Fomalont et al. (1991) found $\beta_{\mathrm{med}} \approx 0.38$ for μJy sources selected at 4.9 GHz. Thus, the host galaxy of GRB 980703 appears to be a normal μJy source compared to sources selected at 4.9 or 8.5 GHz. In addition, it has been noted (Richards 2000) that the spectral index of radio sources selected at frequencies larger than 5 GHz flattens from a value of approximately 0.7 for the mJy ($F_{\nu} \gtrsim 1$ mJy) population to 0.3 for μJy sources.

The reason for the flattening of the spectral index is a varying ratio of thermal bremsstrahlung to synchrotron emission. Supernova remnant shock acceleration of electrons results in synchrotron emission, with a characteristic spectral index of ≈ 0.8 (Condon 1992). On the other hand, thermal bremsstrahlung emission from HII regions, excited by star formation, has a much flatter spectral index, $\beta \approx 0.1$. Thus, as the direct contribution from massive stars increases the spectra are expected to flatten from a value of 0.8 to 0.1. This is exactly the effect that is observed in the aforementioned surveys.

Within the HDF and SSA13 Richards et al. (1999) identified radio sources with fluxes in the range 10–100 μJy with bright disk galaxies with $I \approx 22$ mag. The $I-K$ color for these galaxies is approximately 2.5 mag. Bloom et al. (1998) find $I \approx 21.9$ mag and $I-K \approx 2.1$ mag for the host of GRB 980703. Thus, we see from both the radio spectrum of the source, and the optical I mag and $I-K$ color that the host galaxy of GRB 980703 has the characteristics of a typical star-forming radio galaxy selected at 8.5 GHz.

Figure 3 shows the total SFR in the host galaxy of GRB 980703 as compared to sources in the HDF, its flanking fields, SSA13, and V15 (Haarsma et al. 2000) in the redshift range $0.85-1.15$. These fields have been observed to μJy sensitivities at cm wavelengths, and the detected radio sources have been identified with optical sources for which the redshift was determined. We use the flux and spectral index measurements along with equation 1 and the correction factor to calculate the total SFR. It is clearly seen from the figure that the host of GRB 980703 is an average galaxy at $z \approx 1$ based on star formation. This conclusion meshes well with the comparison of the radio spectral index, optical I mag, and optical $I-K$ color of the host of GRB 980703 to the same sample.

4.2. *Star Formation Rate from Optical and Sub-mm Data*

Djorgovski et al. (1998) used Hα and the 2800A UV continuum to calculate a SFR of approximately 10 $\mathrm{M}_{\odot}$/yr in the host of GRB 980703, after correcting for rest-frame extinction, $A_V \approx 0.3$ mag. Sokolov et al. (2001) found a similar intrinsic extinction, $A_V \approx 0.3-0.65$, and based on template spectral energy distributions found that the best model for the broadband optical spectrum is given by exponentially decreasing star formation with an extinction-corrected SFR of 20 $\mathrm{M}_{\odot}$/yr.

Clearly, the SFR derived from optical indicators is much lower than the value from radio measurements, even after correcting for extinction. This result is part of a general trend that has been observed in galaxies with SFR $\gtrsim 0.1$ $\mathrm{M}_{\odot}$/yr (Hopkins et al. 2001). Hopkins et al. (2001) propose dust reddening dependent on SFR as the solution to this problem, and we therefore expect a much better result if we use their prescription. Extending their correlation to $\mathrm{SFR}_{1.43} \approx 500$ $\mathrm{M}_{\odot}$/yr, we find that the predicted observed SFR from Hα is approximately 70 $\mathrm{M}_{\odot}$/yr. This value is still much higher than the measured SFR. In fact, in the Hopkins et al. (2001) sample the optically-derived SFR rarely exceeds 10 $\mathrm{M}_{\odot}$/yr, while the radio-derived values go up to several hundred $\mathrm{M}_{\odot}$/yr, indicating that the optical emission does not trace the entire star-forming volume. Thus, the SFR values for this particular galaxy are not unexpected.

The sub-mm (e.g. 350 GHz) emission from galaxies serves as another estimator of SFR, and it is related to the radio emission at 1.43 GHz via a redshift-dependent spectral index, $\beta_{1.4}^{350}$ (Carilli & Yun 1999, 2000; Dunne, Clements & Eales 2000). Using the calibration of Dunne, Clements & Eales (2000) we find a value of $\beta_{1.4}^{350} \approx 0.6 \pm 0.1$ at $z \approx 1$, which gives $F_{\nu}(350) \approx 1.9^{+1.4}_{-0.8}$ mJy. Observations with the Sub-millimeter Common User Bolometer Array (SCUBA) camera on the James Clark Maxwell Telescope (JCMT) 12.4 days after the burst provided a 2σ upper limit of 3.2 mJy on the combined emission from the afterglow and host at 350 GHz (Smith et al. 1999), consistent with the predictions from the radio–sub-mm relation.

To conclude, we use the derived SFR to calculate the expected far-IR (FIR) emission from the host of GRB 980703. The luminosity of the FIR radiation can be derived from the empirical relation suggested by Helou, Soifer & Rowan-Robinson (1985),

$$q = -12.6 + \log(F_{FIR}/F_{1.4}) \approx 2.3 \quad (2)$$

which evaluates to $L_{FIR} \approx 10^{12}$ $\mathrm{L}_{\odot}$ for the host of GRB 980703;

here F_{FIR} is the total flux in the range 40–120 μm in units of erg sec^{-1} cm^{-2}, and $F_{1.4}$ is the flux density at 1.4 GHz in units of erg sec^{-1} cm^{-2} Hz^{-1}. Hopkins et al. (2001) provide the calibration $L_{FIR} = 5.81 \times 10^9 \times$ SFR L$_{\odot}$, which gives $L_{FIR} \approx 3 \times 10^{12}$ L$_{\odot}$, in good agreement with the previous value. These values of the FIR luminosity place the host galaxy of GRB 980703 in the category of ULIRG (Sanders & Mirabel 1996).

5. OFFSET MEASUREMENTS AND SOURCE SIZE

Figure 4 shows the projected angular offset between the host galaxy and afterglow of GRB 980703, for each individual detection, and the combined value from all observing runs (insert in Figure 4). Positions are determined from Gaussian fits, and the host-GRB offset is calculated with respect to a Very Long Baseline Array (VLBA) position that was measured to 0.0007 arcsec accuracy in each coordinate on 1998 August 2 at 8.42 GHz (Berger et al. 2001).

We find an average offset from all measurements of -0.032 ± 0.015 arcsec in RA and 0.024 ± 0.015 arcsec in declination. The uncertainty in the position of the source is given by $\delta\theta_{\rm offset} \approx (\theta_{synbeam}/2)/(S/N)$, where $\theta_{synbeam} \approx \lambda/B_{max}$ is the half-power synthesized beam-width, λ is the observing wavelength, B_{max} is the length of the maximum baseline, and S/N is the signal-to-noise ratio of the flux measurement.

The optical measurements of Bloom, Kulkarni & Djorgovski (2000) for the host of GRB 980703, give an angular offset of -0.054 ± 0.055 in RA and 0.098 ± 0.065 in declination (see insert in Figure 4). They conclude that GRB 980703 was not significantly offset from the center of its host galaxy, in agreement with the more accurate offset measurements in the radio.

In addition to accurate measurements of the offset, the radio observations allow us to place meaningful limits on the size of the radio-emitting region (i.e. the size of the star-forming region). We find that in our highest resolution images the source is unresolved, and therefore, based on the synthesized beam size we can derive an upper limit on the physical size of the source. For our adopted cosmological parameters (section 4) we find that the angular diameter distance to the source is $d_A \approx 5.4 \times 10^{27}$ cm. The full synthesized beam-width at 8.46 GHz is $\theta_{HPBW} \approx 0.27$ arcsec, which gives an upper limit of $D_{rad} = d_A \theta_{HPBW} < 2.3$ kpc on the diameter of the source.

Holland et al. (2001) used a $R^{1/n}$ profile to fit the optical emission from the host and found that the best fit gives a half-light radius of 0.13 arcsec, which corresponds to an exponential disk with a scale-diameter of 0.44 arcsec. Thus, the physical size of the galaxy is $D_{opt} \approx 3.7$ kpc, 60% larger than the upper limit from our radio measurements. However, Holland et al. (2001) claim that the center of the galaxy is 0.2 mag bluer than the outer regions of the host. If so, star formation must be mainly taking place within the inner parts of the galaxy. Since the radio emission directly traces current star formation, we expect the radio emission to be more centrally concentrated than the optical emission. Thus, as expected, the radio size of the galaxy is smaller than the optical size.

Most likely the GRB is located within the nuclear starburst given the small offset of the GRB from the centroid of the galaxy. If so it raises the question of why the afterglow was not completely extinguished by dust. In fact, in order to reconcile the optical and radio derived SFRs we require a rest-frame extinction of $A_V \sim 4.5$ mag. Observations of the afterglow, which provide an estimate of extinction along the line-of-sight to the burst, give values of 1–2 mags from optical observations, and somewhat higher values from X-ray observations (Bloom et al. 1998; Castro-Tirado et al. 1999; Vreeswijk et al. 1999). Thus, the extinction in the nuclear star-forming region is higher than the average over the whole galaxy, and the correction to the observed optical SFR is almost sufficient to reconcile it with the value of 500 M$_{\odot}$/yr derived from the radio.

The relatively small source size also agrees well with the classification of the host of GRB 980703 as a ULIRG exhibiting a starburst. Kennicutt (1998, and references therein) showed that star formation with a rate $\gtrsim 20$ M$_{\odot}$/yr invariably takes place in circumnuclear regions of size 0.2–2 kpc, in the form of nuclear starburst. As a result, we expect that ULIRGs will have such size scales when traced by star formation, and the source size we measured for the host of GRB 980703 indicates that it is probably undergoing a nuclear starburst.

Finally, from the source size and offset measurement we conclude that GRB 980703 took place in the region of maximum star formation, providing further indirect evidence linking GRBs to massive stars

6. CONCLUSIONS

Late-time observations of GRB 980703 reveal a steady component, with a flux density $F_{\nu,1.43} = 68.0 \pm 6.6$ μJy and a spectral index $\beta = 0.32 \pm 0.12$. The spectral and temporal characteristics of this emission indicate that it does not arise from the afterglow itself, but rather it is the result of star formation in the host galaxy, with SFR ≈ 500 M$_{\odot}$/yr. This leads to the interpretation that this host galaxy is a ULIRG undergoing a starburst. In addition, the star formation is concentrated within the inner two kpc of the host, and the progenitor of GRB 980703 was positioned within this region of star formation. This conclusion lends additional support for the collapsar model.

If GRBs really come from massive stars, then they can be used to trace the star formation history of the universe (e.g. Blain & Natarajan 2000). In addition, GRBs and their afterglows are potentially detectable out to very high redshifts (Lamb & Reichart 2000). These propositions, taken together with the dust-penetrating power of their γ-ray emission, make GRBs a unique tool for the study of galaxies and the IGM over a wide redshift range. In particular, radio and sub-mm/FIR observations of a GRB-selected galaxy sample will be extremely useful for the study of the obscured star formation fraction, and the properties of starbursts at high redshifts. Moreover, a comparison of the global star formation history as derived from these long-wavelength host studies, with the redshift distribution of GRBs, will provide valuable insight as to how well GRBs trace the formation rate of massive stars; we expect that if GRBs trace only a particular channel of star formation, the two distributions will not agree.

Therefore, it is imperative to study the hosts of GRBs in the radio and sub-mm/FIR. Future observatories such as the Space Infrared Telescope Facility (SIRTF; to be launched in July 2002), the Expanded VLA (EVLA), and the Square-Kilometer Array (SKA) will allow detailed studies of these hosts. In the FIR, SIRTF will have the ability to detect sources down to a few mJy, allowing the detection of galaxies with SFR comparable to that in the host of GRB 980703 out to $z \sim 10$; alternatively, we will be able to detect hosts with SFR as low as a few M$_{\odot}$/yr at $z \sim 1$. The EVLA and SKA will greatly improve the detectability of host galaxies in the radio, and will also allow much higher angular resolution studies of compact star-forming regions. With a factor ten increase in resolution and a factor five increase in sensitivity over the current VLA, we will be able to probe scales of approximately 5 mas with the EVLA; for a galaxy at $z \approx 1$ this translates to a physical scale of 150 pc. In addition, EVLA will detect galaxies with a total SFR as low as 50 $M_{\odot}$/yr at $z \sim 1$. The SKA, with a similar resolution, but a much larger collecting area, will extend this capability to even lower SFR and smaller star-forming regions.

Thus, as more host galaxies are detected and studied in detail in the radio and sub-mm/FIR, we will be able to address a large number of issues pertaining not only to the bursts themselves, but also to the characteristics of galaxies at high redshifts.

We acknowledge support by NSF and NASA grants.

REFERENCES

Barger, A. J., Cowie, L. L., & Richards, E. A. 2000, AJ, 119, 2092.
Berger, E., et al. 2001, in preparation.
Blain, A. W. & Natarajan, P. 2000, MNRAS, 312, L35.
Bloom, J. S., et al. 1998, ApJ, 508, L21.
Bloom, J. S., Kulkarni, S. R., & Djorgovski, S. G. 2001, submitted to AJ. astro-ph/0010176.
Carilli, C. L. & Yun, M. S. 1999, ApJ, 513, L13.
Carilli, C. L. & Yun, M. S. 2000, ApJ, 530, 618.
Castro-Tirado, A. J., et al. 1999, ApJ, 511, L85.
Chevalier, R. A. & Li, Z. 2000, ApJ, 536, 195.
Condon, J. J. 1992, ARA&A, 30, 575.
Djorgovski, S. G., et al. 2001, in preparation.
Djorgovski, S. G., et al. 1998, ApJ, 508, L17.
Dressler, A. & Gunn, J. E. 1982, ApJ, 263, 533.
Dunne, L., Clements, D. L., & Eales, S. A. 2000, MNRAS, 319, 813.
Falcke, H., et al. 2000, to appear in "Probing the Physics of Active Galactic Nuclei by Multiwavelength Monitoring", eds. B.M. Peterson, R.S. Polidan, & R.W. Pogge, ASP Conf. Ser. astro-ph/0009457.
Fomalont, E. B., et al. 1991, AJ, 102, 1258.
Frail, D. A., Waxman, E., & Kulkarni, S. R. 2000, ApJ, 537, 191.
Galama, T. J. & Wijers, R. A. M. J. 2000, ApJ in press; astro-ph/0009367.
Haarsma, D. B., et al. 2000, ApJ, 544, 641.
Helou, G., Soifer, B. T., & Rowan-Robinson, M. 1985, ApJ, 298, L7.
Holland, S. et al. 2001, submitted to A&A. astro-ph/0103058.
Hopkins, A. M., et al. 2001, accepted to AJ. astro-ph/0103253.
Kennicutt, R. C. 1992, ApJ, 388, 310.
Kennicutt, R. C. 1998, ARA&A, 36, 131.
Lamb, D. Q. & Reichart, D. E. 2000, ApJ, 536, 1.
Richards, E. A. 2000, PASP, 112, 1001.
Richards, E. A., et al. 1999, ApJ, 526, L73.
Rola, C. S., Terlevich, E., & Terlevich, R. J. 1997, MNRAS, 289, 419.
Sanders, D. B. & Mirabel, I. F. 1996, ARA&A, 34, 749+.
Sari, R., Piran, T., & Halpern, J. P. 1999, ApJ, 519, L17.
Sari, R., Piran, T., & Narayan, R. 1998, ApJ, 497, L17.
Smith, I. A. et al. 1999, A&A, 347, 92.
Sokolov, V. V. et al. 2001, submitted to A&A; astro-ph/0104102.
Vreeswijk, P. M. et al. 1999, ApJ, 523, 171.
Windhorst, R. A. et al. 1993, ApJ, 405, 498.

TABLE 1
RADIO OBSERVATIONS OF GRB 980703

Epoch (UT)	Δt (days)	Array Configuration	$t^{\mathrm{on-source}}$ (hrs)	ν_0 (GHz)	S$\pm\sigma$ (μJy)
1999 June 15.36—26.29	352.65	A	6.5	1.43	81$\pm$18
1999 July 10.53—28.28	381.22	A	13.4	1.43	57$\pm$10
1999 August 19.40—September 21.24	428.64	A	11.3	8.46	37$\pm$8
1999 November 24.06	508.88	B	1.7	1.43	57$\pm$20
2000 March 5.70	610.52	BnC	2.8	8.46	57$\pm$14
2000 October 7.30—November 19.08	847.01	A	6.5	1.43	76$\pm$11
2000 December 2.19—4.97	882.60	A	4.9	4.86	35$\pm$11
2000 December 21.15—2001 January 4.98	908.38	A	7.0	8.46	41$\pm$8
2001 February 2.00—4.93	945.29	AnB	1.9	1.43	113$\pm$21
2001 February 8.08	949.90	AnB	1.2	4.86	57$\pm$28
2001 March 2.98—9.00	975.81	B	4.5	4.86	43$\pm$15
2001 March 22.96—April 8.56	1001.08	B	2.6	1.43	83$\pm$30

NOTE.—The columns are (left to right), (1) UT date of the start of each observation or range of dates for observations which were added over several days, (2) time elapsed since the γ-ray burst, (3) array configuration, (4) total on-source observing time, (5) observing frequency, and (6) peak flux density at the best fit position of the radio transient, with the error given as the root mean square noise on the image.

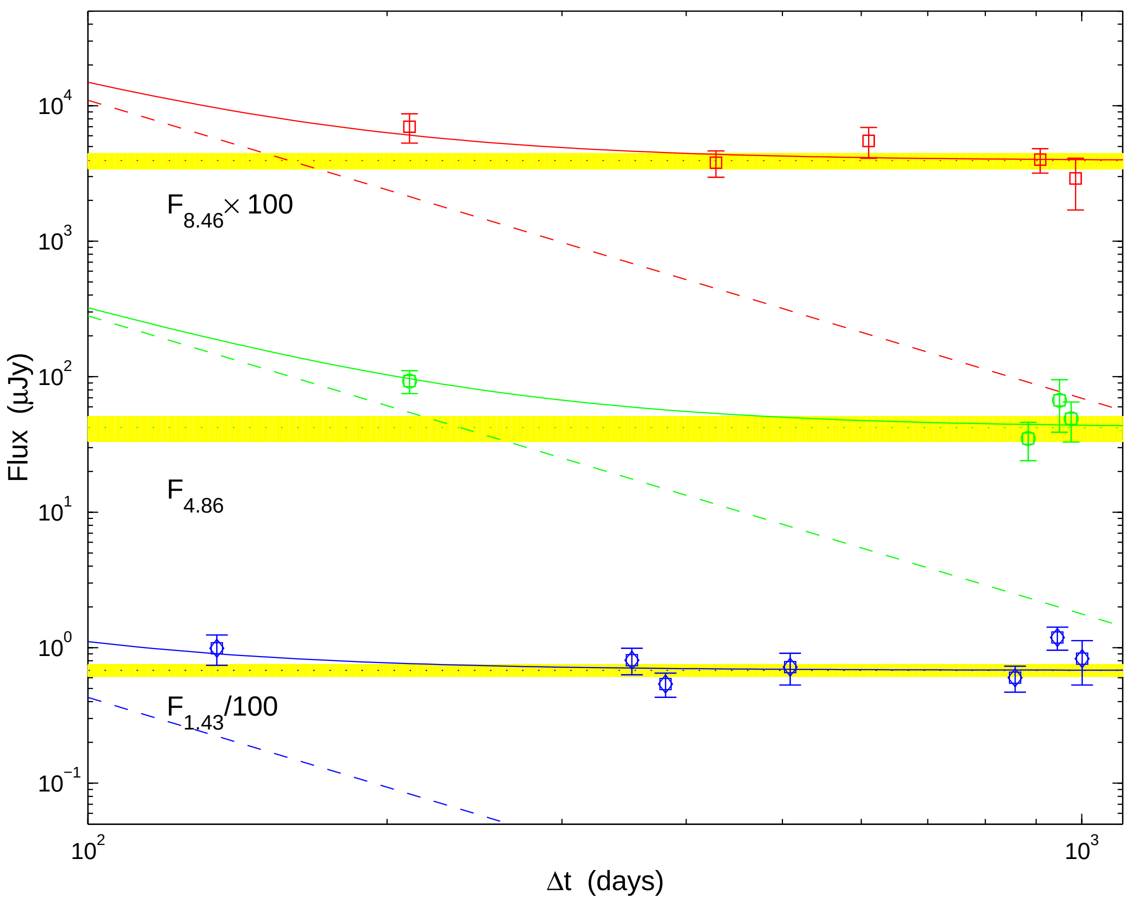

FIG. 1.— Radio lightcurves at 1.43, 4.86, and 8.46 GHz. The thin solid lines are the combined afterglow and host galaxy emission, the dotted lines indicate the afterglow emission, and the thick solid lines are the weighted-average fluxes of the host galaxy, with the thickness indicating the uncertainty in the flux. Only measurements at $t \gtrsim 350$ days after the burst were used to calculate the host flux. The fits are based on broadband fitting (Berger et al. 2001). The data clearly indicate that there is a constant component in the observed emission, interpreted as the host galaxy. For details of the data reduction and analysis see section 2.

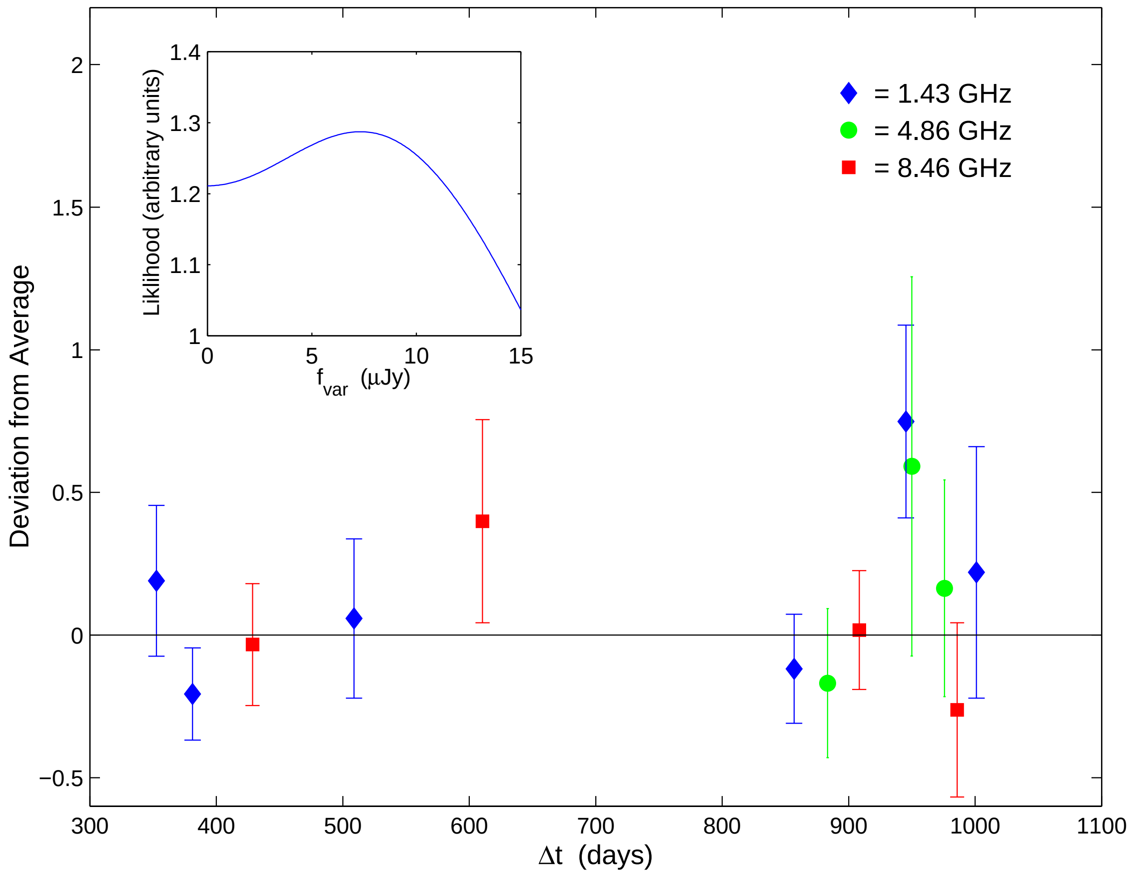

FIG. 2.— Fluctuations of individual measurements around the weighted average presented by the wide strips in figure 1. We note that there are no fluctuations above 1.1σ at 8.46 GHz, 0.8σ at 4.86 GHz, and 1.7σ at 1.43 GHz, indicating that the flux in each band is consistent with a constant. In fact, if we assume that the source has some variability (over that due to measurement errors), then the variable flux is less than ± 7 μJy, with a 40% probability that there are no fluctuations at all (see insert). This conclusion supports the hypothesis that the radio emission is not due to an AGN.

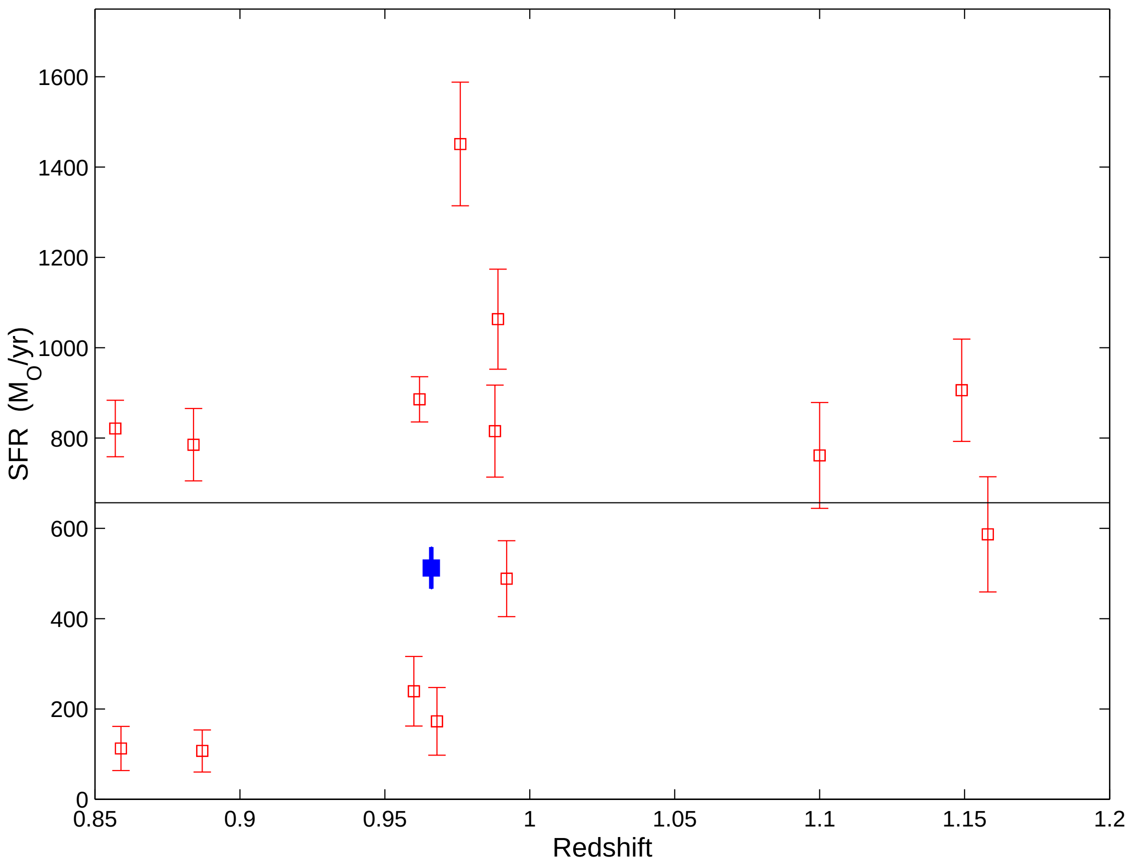

FIG. 3.— SFR for radio galaxies in the HDF, SSA13 and V15 (Haarsma et al. 2000) in the redshift range 0.85–1.15. The dashed line is an average over this redshift range. The host galaxy of GRB 980703 is marked by a solid square. The errorbars on the survey sources indicate a 10 μJy measurement error. The host of GRB 980703 appears to be an average star-forming galaxy relative to the sample.

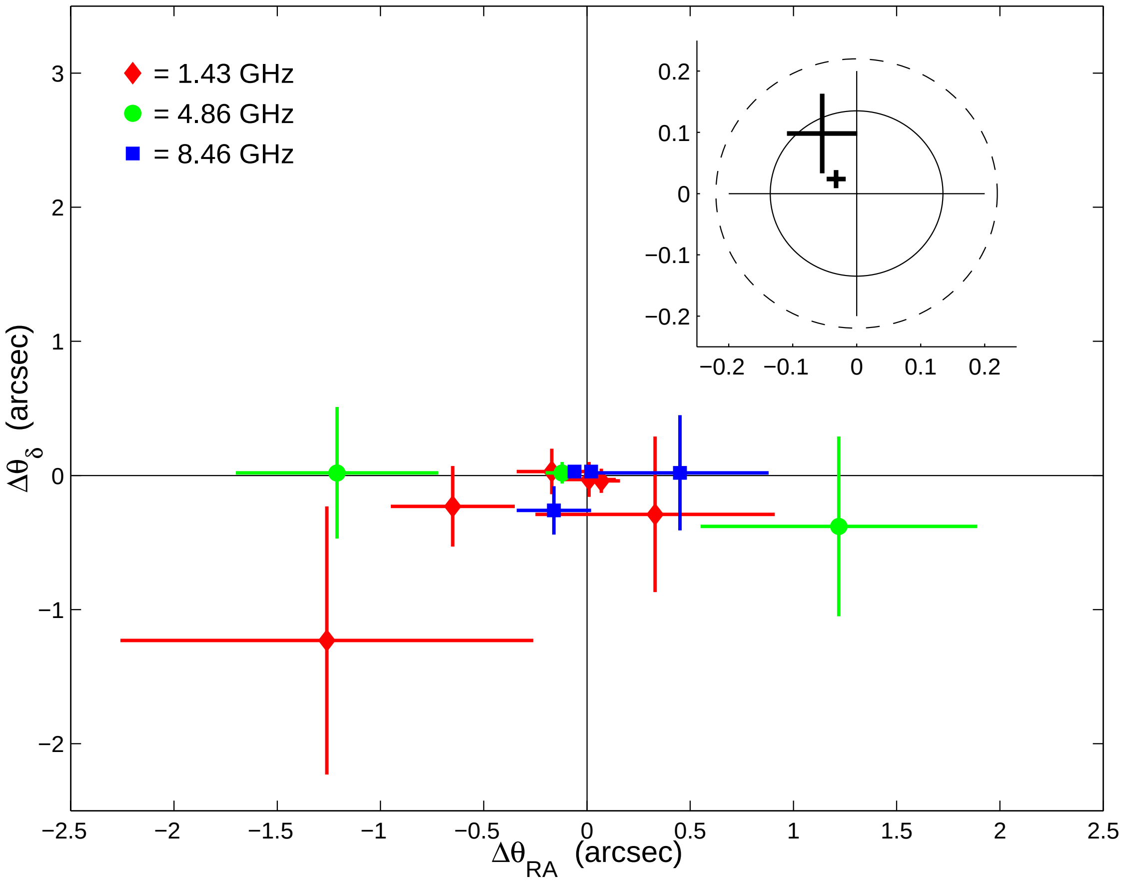

FIG. 4.— Offset measurements for all epochs in which the host galaxy emission dominates. The plot shows the offset in RA and δ of the VLBA position of the burst (see section 5) relative to the host center, $(\Delta\theta_{\rm RA}, \Delta\theta_{\delta})$=(0,0). The most accurate measurements are at 8.46 GHz in the VLA A configuration. In this mode we achieved an rms positional error of 0.02 arcsec. The insert shows the weighted average offset in both RA and δ (small cross). The larger cross is the offset measurement from Bloom, Kulkarni, and Djorgovski (2001). The solid circle designates the projected maximum source size from the radio observations in the A configuration at 8.46 GHz, and the dashed circle is the optical size from Holland et al. (2001). Clearly the formation of massive stars is concentrated in the central region of the host. The small offset of the burst from the host center indicates that GRB 980703 occurred in the region of maximum star formation, which points to a link between GRBs and massive stars.

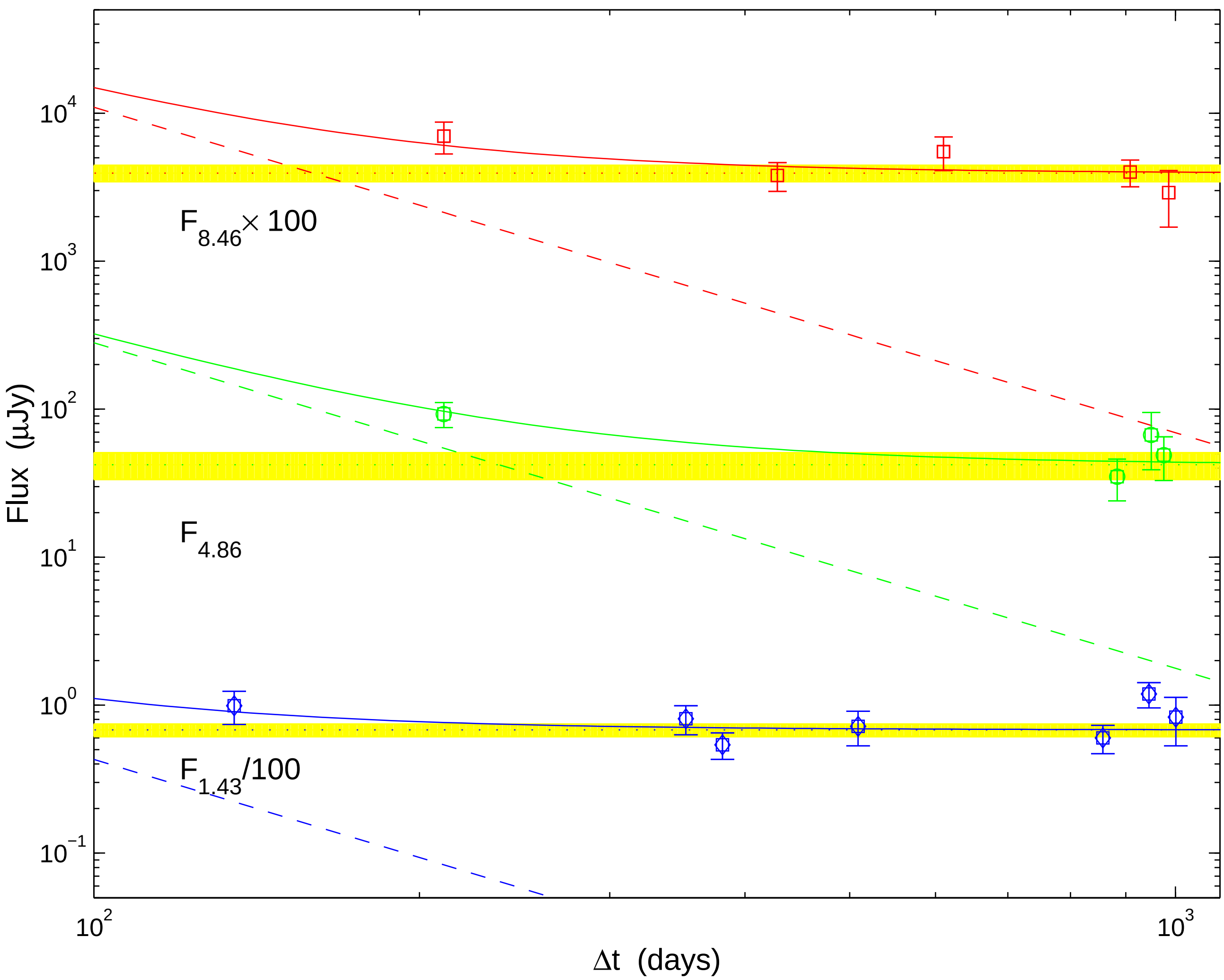

Flux (μJy)
10^4
10^3
10^2
10^1
10^0
10^{-1}
$F_{8.46}\times 100$
$F_{4.86}$
$F_{1.43}/100$
10^2
10^3
Δt (days)

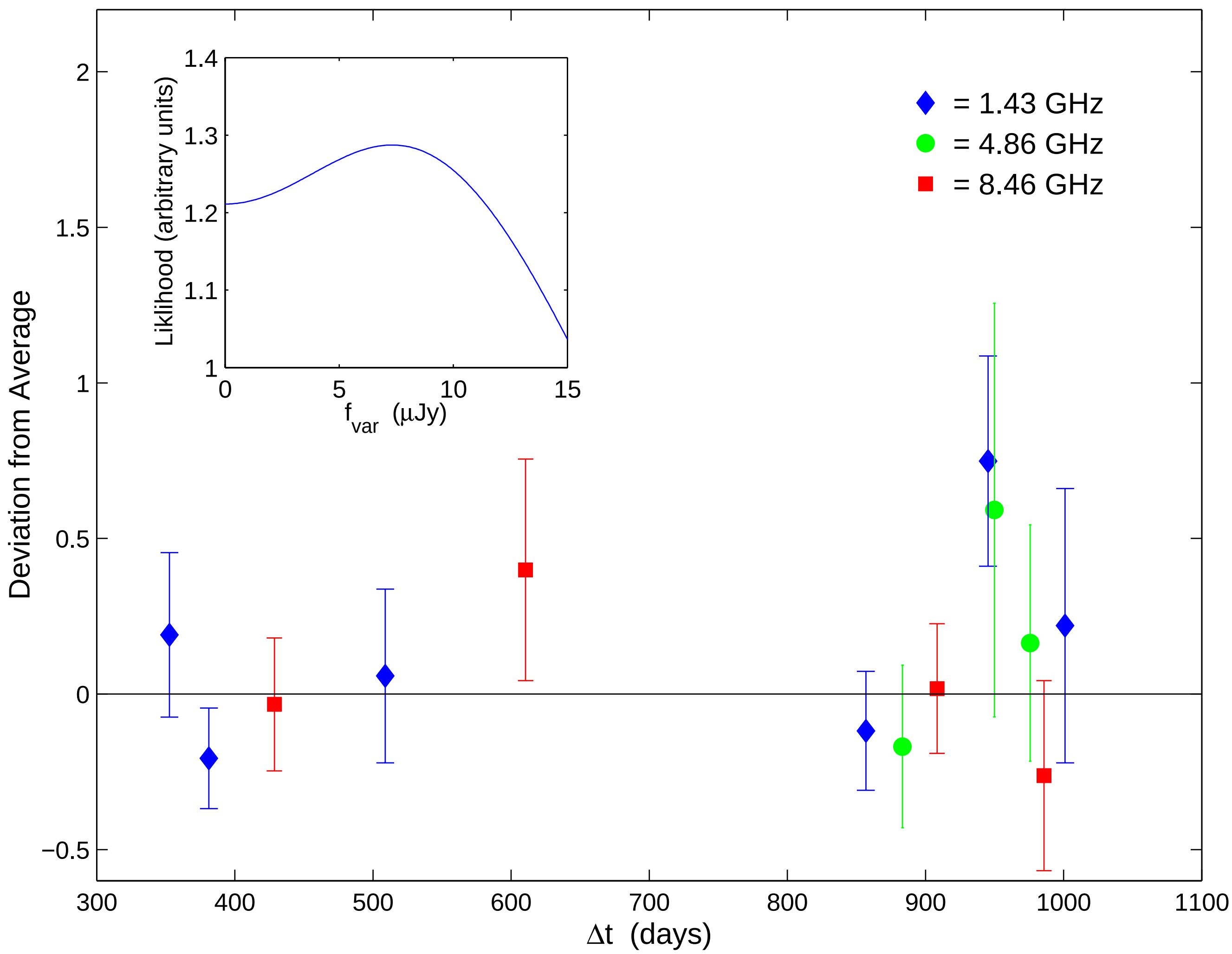

= 1.43 GHz
= 4.86 GHz
= 8.46 GHz
Deviation from Average
Δt (days)
Liklihood (arbitrary units)
f_{var} (μJy)

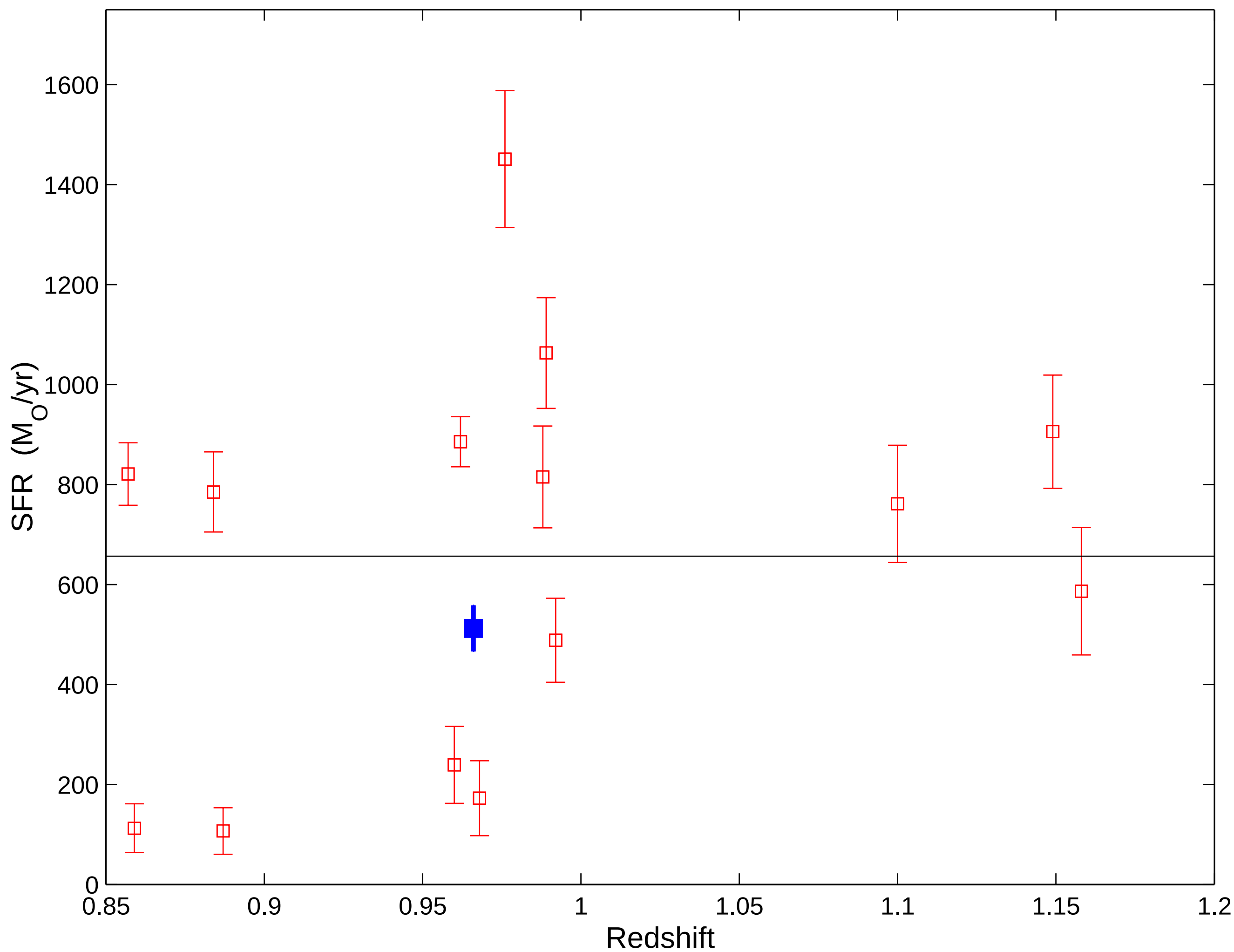

SFR (M_O/yr)
0
200
400
600
800
1000
1200
1400
1600
0.85
0.9
0.95
1
1.05
1.1
1.15
1.2
Redshift

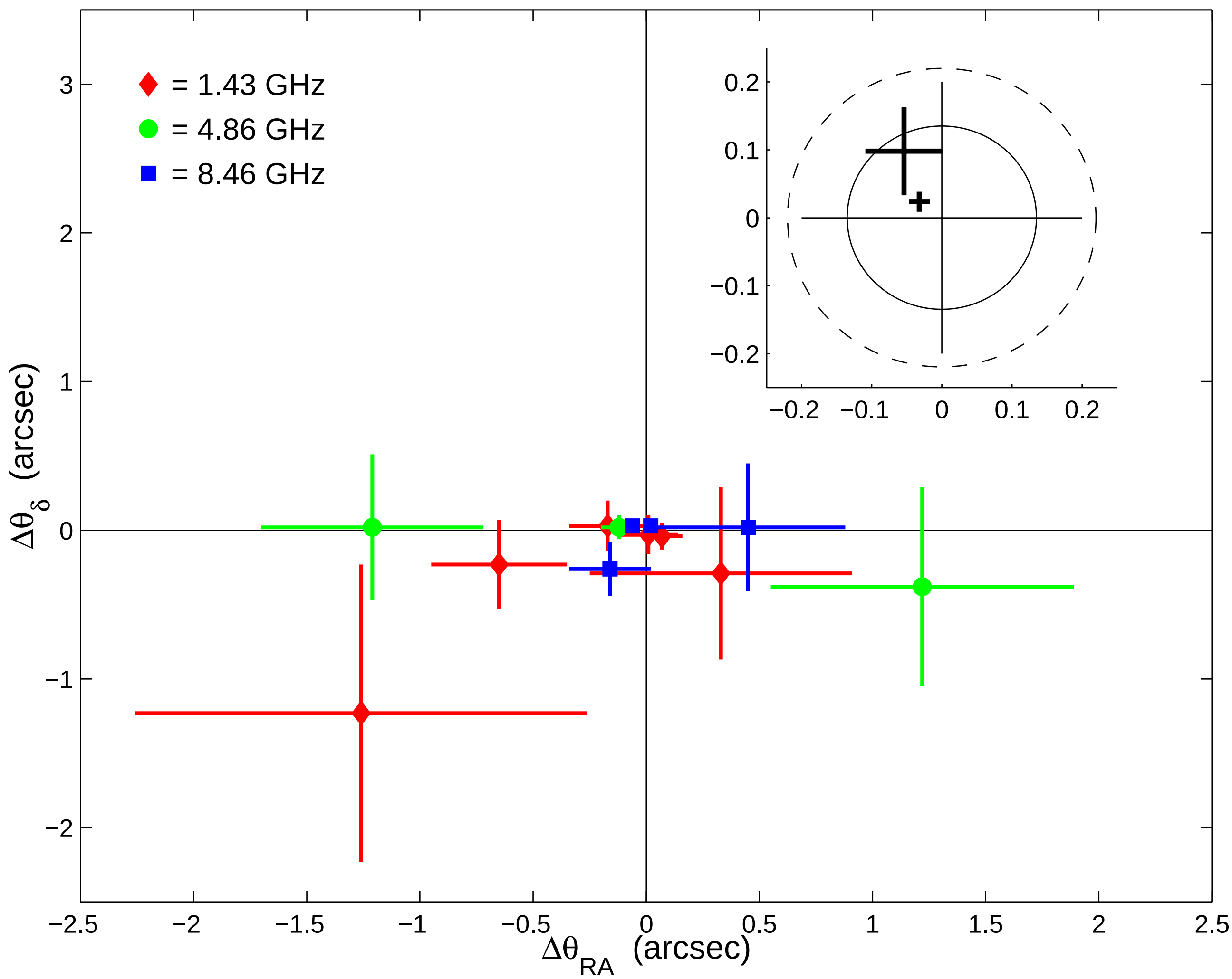

= 1.43 GHz
= 4.86 GHz
= 8.46 GHz
$\Delta\theta_{\delta}$ (arcsec)
$\Delta\theta_{RA}$ (arcsec)